AJNR

Quantification of Brain Damage in Cerebrotendinous Xanthomatosis with Magnetization Transfer MR Imaging

Matilde Inglese, Nicola DeStefano, Elisabetta Pagani, Maria T. Dotti, Giancarlo Comi, Antonio Federico and Massimo Filippi

AJNR Am J Neuroradiol 2003, 24 (3) 495-500
http://www.ajnr.org/content/24/3/495

Quantification of Brain Damage in Cerebrotendinous Xanthomatosis with Magnetization Transfer MR Imaging

Matilde Inglese, Nicola De Stefano, Elisabetta Pagani, Maria T. Dotti, Giancarlo Comi, Antonio Federico, and Massimo Filippi

BACKGROUND AND PURPOSE: **Conventional MR imaging for quantification of brain damage in monitoring the evolution of cerebrotendinous xanthomatosis (CTX) has limitations. Magnetization transfer (MT) MR imaging is overcoming these limitations. Using MT MR imaging, we sought to quantify, in vivo, the extent of brain and cerebellar damage in patients with CTX, with the ulimate goal to investigate the magnitude of the correlation between MT MR imaging findings and clinical disability.**

METHODS: **Conventional and MT MR images of the brain were obtained in nine patients with CTX and in 10 sex- and age-matched healthy volunteers. MT ratio histograms were derived of the whole brain, brain normal-appearing white matter (NAWM), brain normal-appearing gray matter (NAGM), cerebellar NAWM, and cerebellar NAGM. Clinical disability was measured by using the Expanded Disability Status Scale (EDSS).**

RESULTS: **Average MT ratio and peak heights of the whole brain, brain NAWM, and brain NAGM histograms in patients with CTX were significantly lower than the corresponding quantities in the control subjects. All cerebellar NAGM MT ratio histogram–derived metrics and average MT ratio of the cerebellar NAWM histogram in patients with CTX were also significantly lower than the corresponding quantities in the control subjects. Strong correlations were found between the EDSS score and a composite whole-brain MT ratio histogram score ($r = 0.77$, $P < .01$) and a composite brain white matter MT ratio histogram score ($r = 0.71$, $P < .03$). A strong correlation was also found between the cerebellar functional system score and a composite cerebellar NAWM score ($r = 0.72$, $P < .02$).**

CONCLUSION: **The quantitative assessment of brain damage in patients with CTX with use of MT MR imaging can provide powerful measures of disease outcome.**

Cerebrotendinous xanthomatosis (CTX) is a rare, autosomal recessive disorder due to a deficiency of the mitochondrial enzyme 27-sterol hydroxylase (CYP27) (1, 2). This causes an impairment of the metabolic pathway of cholesterol, resulting in an excessive production of cholestanol, which then accumulates in many tissues (3, 4). Although the clinical manifestations of CTX can be secondary to damage of multiple organ systems (1, 4), they are usually dominated by the classical triad of the disease, which consists of premature bilateral cataracts, tendon xanthomas, and neurologic abnormalities (1, 4).

In patients with CTX, several studies with use of conventional MR imaging have shown diffuse and focal abnormalities of the white matter, cerebral and cerebellar atrophy, and a typical abnormal MR signal intensity change of the dentate nuclei and the surrounding white matter (5–9). A recent proton MR spectroscopy study also showed that the brain damage in patients with CTX extends well beyond the abnormalities seen on conventional MR images in both the supratentorial and infratentorial compartments (9).

In clinical neurology, in vivo quantification of brain damage with use of MR-based technology is becoming an important component in monitoring the evolution of several diseases (10). This is particularly true when disease-modifying treatments are available, as is the case with CTX, for which treatment with che-

Received March 22, 2002; accepted after revision August 27.

From the Neuroimaging Research Unit, Department of Neuroscience (M.I., E.P., M.F.) and the Department of Neurology (G.C.), Scientific Institute and University Ospedale San Raffaele, Milan, Italy, and the Neurometabolic Unit, Institute of Neurological Sciences, University of Siena, Siena, Italy (N.D.S., M.T.D., A.F.).

Address reprint requests to Massimo Filippi, MD, Neuroimaging Research Unit, Department of Neuroscience, Scientific Institute and University Ospedale San Raffaele, Via Olgettina, 60, 20132 Milan, Italy; e-mail: m.filippi@hsr.it

nodeoxycholic acid alone or in combination with 3-hydroxy-methyglutaryl coenzyme A reductase inhibitors has been shown to slow or even reverse the progression of the disease (11–13). In this context, outcome measures derived from conventional MR imaging have two major limitations. First, abnormalities seen on conventional MR images provide a nonspecific measure of the overall extent of macroscopic tissue damage (10). Second, given the presence of diffuse white matter abnormalities (5–9) and damage of the normal-appearing tissues (9) in patients with CTX, conventional MR imaging outcomes would inevitably provide inaccurate estimates of the actual tissue damage. Although proton MR spectroscopy enables us to obtain important pieces of information about axonal and mitochondrial dysfunction (9), it does not allow (with most of the current techniques) complete brain coverage, with the possibility of sampling and repositioning errors in serial studies, which are needed to monitor treatment efficacy.

Magnetization transfer (MT) MR imaging can go some way toward overcoming these limitations. A low MT ratio indicates a reduced capacity of the protons in the brain tissue matrix to exchange magnetization with the surrounding water protons, and in a postmortem study of individuals with multiple sclerosis, a low MT ratio was found to be strongly associated with the degree of myelin and axon loss (14). In addition, estimates of the amount and severity of tissue damage of the whole brain can be obtained by using MT ratio histogram analysis (15). Previous studies found that MT ratio histogram-derived metrics correlated with clinical disability and cognitive impairment in demyelinating (15–17), vascular (18, 19), and degenerative (20) diseases of the central nervous system. Against this background and with the ultimate goal to define new putative markers for monitoring CTX evolution, we performed this study based on MT ratio histogram analysis to quantify the overall extent of macroscopic and microscopic brain damage, to define the extent of gray and white matter damage in the brain and the cerebellum, and, most important, to investigate the magnitude of the correlation between MT MR imaging findings and clinical status of the patients.

Methods

Patients

Nine adult patients with CTX (five women, four men; mean age, 39.1 years; range, 32–53 years) from seven families and 10 sex- and age-matched healthy volunteers (six women, four men; mean age, 41.7 years; range, 26–56 years) were studied. All patients met the clinical criteria for CTX and had a blood level of cholestanol greater than 1 mg/dL. DNA point mutations or deletions in the *CYP27* gene were detected in all patients. A complete clinical evaluation was performed on the day of the MR imaging examination by an experienced neurologist (A.F.) who was unaware of the MR imaging results, and the patients' clinical disability was assessed by using the Expanded Disability Status Scale (EDSS) (21). At the time of the clinical and MR imaging examinations, all patients showed the classic triad of the disease. Patients with CTX had been treated with chenodeoxycholic acid for several years. Local ethics committee approval and written informed consent from all subjects were obtained before study initiation.

MR Image Acquisition

Brain MR images were obtained by using a Gyroscan NT operating at 1.5 T (Philips Medical Systems, Best, the Netherlands). During a single session, the following pulse sequences were obtained in all subjects: dual-echo fast spin-echo (2800/20, 120/1 [TR/TE/excitations], echo train length of 5), and 2D gradient-echo (640/12/2, flip angle of 20°) with and without the standard manufacturer's off-resonance radio-frequency saturation pulse. For both sequences, 22 contiguous axial sections were acquired with 5-mm section thickness, 256 × 256 matrix, and 250 × 250-mm field of view. The sections were positioned to run parallel to a line that joins the most inferoanterior and inferoposterior parts of the corpus callosum.

MR Image Analysis and Postprocessing

Dual-echo images from all subjects were reviewed in a random order and without knowledge of the subject's identity by two experienced observers (M.I., M.F.) by consensus to identify the presence of hyperintense white matter (focal or diffuse) and dentate nuclei abnormalities. Hyperintense lesion volume on proton density–weighted images was measured as described previously (16). These observers also assessed whether cerebral or cerebellar atrophy was present, and, when detected, atrophy was scored as mild, moderate, or severe.

Brain MT ratio histograms were obtained as follows. First, the two gradient-echo images (ie, with and without the MT saturation pulse) were coregistered. Registration was performed by using an automated technique based on pixel similarity measures (22). Next, an MT ratio image was calculated from the coregistered gradient-echo images as previously described (16). Brain MT ratio maps were then coregistered with the dual-echo proton density–weighted images (23). The entire brain was segmented from the MT ratio images by a single observer (M.I.), without knowledge of the subject's identity, by using a segmentation technique based on local thresholding (24). Finally, MT ratio histograms (with bins 1% in width) were produced. We excluded from the analysis all the pixels with MT ratios lower than 10%, to minimize partial-volume effects from the CSF. To correct for the between-patient differences in brain volumes, each histogram was normalized by dividing it by the total number of pixels included. MT ratio histograms were produced from the whole of the brain tissue and from brain and cerebellar normal-appearing white matter (NAWM) and brain and cerebellar normal-appearing gray matter (NAGM) in isolation. To obtain the MT ratio histograms of NAWM and NAGM, hyperintense lesion outlines from proton density–weighted images were automatically transferred onto the coregistered MT ratio maps and then masked out, as extensively described elsewhere (23). By using the statistical parametric mapping program SPM99 and maximum image inhomogeneity correction (25), brain and cerebellar gray matter, white matter, and CSF were automatically segmented from proton density– and T2-weighted images. Each pixel was classified as gray matter, white matter, or CSF depending on which mask had the greatest probability (maximum likelihood) at that location. This generated mutually exclusive masks for each tissue. The resultant masks were superimposed onto the MT ratio maps on which hyperintense lesions were masked out and the corresponding MT ratio histograms of NAWM and NAGM were produced. For each histogram, the average MT ratio, the peak height (ie, the proportion of pixels at the most common MT ratio), and the peak position (ie, the most common MT ratio) were measured. The average lesion MT ratio was calculated as described previously (16).

TABLE 1: Mean MT ratio histogram-derived metrics of whole-brain tissue, NAWM, and NAGM for the nine patients with CTX and the 10 control subjects

Variable	Control Subjects	Patients with CTX	*P* Value*
Whole brain			
MT ratio (%)	58.0 (0.5)	56.2 (1.4)	.005
MT ratio peak height†	82.9 (7.4)	73.2 (7.0)	.006
MT ratio peak position (%)	60.3 (0.6)	59.8 (1.2)	NS
NAWM			
MT ratio (%)	63.4 (0.4)	62.2 (1.3)	.01
MT ratio peak height†	171.9 (18.5)	134.7 (17.8)	<.001
MT ratio peak position (%)	60.8 (0.4)	60.5 (1.0)	NS
NAGM			
MT ratio (%)	58.1 (0.9)	55.4 (2.2)	.003
MT ratio peak height†	92.1 (13.0)	67.8 (14.1)	.001
MT ratio peak position (%)	56.1 (0.8)	55.7 (1.0)	NS

Note.—Numbers in parentheses are SD.

* NS indicates not significant.

† These data are normalized pixel count.

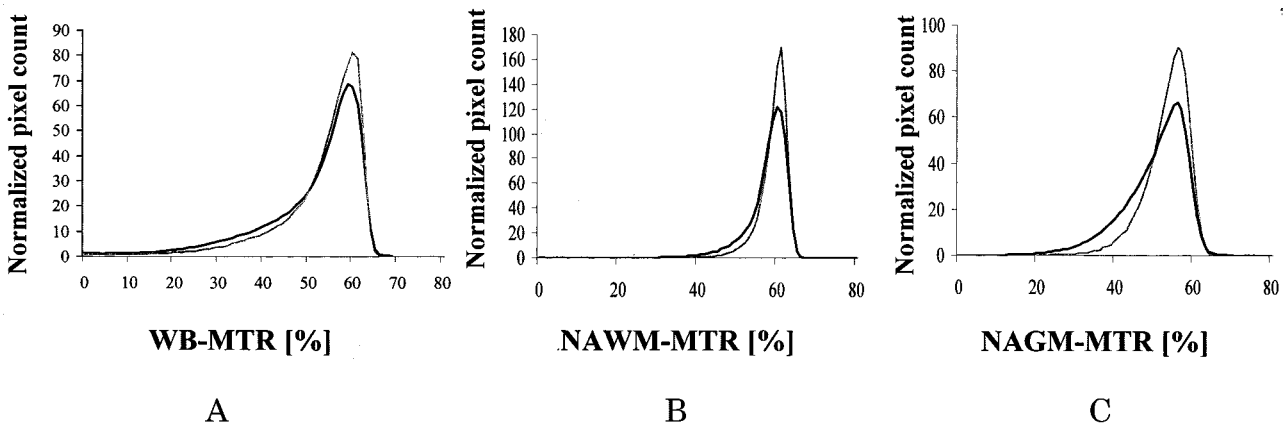

FIG 1. *A–C,* MT ratio (*MTR*) histograms from patients with CTX (black line) and healthy volunteers (gray line) for whole brain (*WB*) (*A*), brain NAWM (*B*), and brain NAGM (*C*).

Statistical Analysis

A two-tailed Student's *t* test for nonpaired data was used to compare MT ratio histogram–derived metrics from the patients with CTX with those from the healthy volunteers. To reflect the large number of statistical comparisons and to avoid type II errors, a *P* value of less than or equal to .01 was considered to indicate a significant difference. To avoid a large number of correlations, multivariable linear regression models were used to generate composite MT ratio histogram–derived scores. Each score was computed by using a linear combination of the three MT ratio–derived metrics of the various histograms. The weight of each MT ratio histogram–derived metrics resulted from the coefficients estimated by the regression model. The magnitude and the significance of the correlations between EDSS scores or the cerebellar functional system scores and composite MT ratio scores were evaluated by a nonparametric Spearman correlation analysis, because EDSS does not satisfy the assumptions of continuity and normality for a valid inference in linear regression models, and the sample size studied was too small for asymptotic properties to be applied. The Spearman rank correlation coefficient was also used to assess the correlations between EDSS scores and lesion volumes or average lesion MT ratio.

Results

In the nine patients with CTX, the mean volume of hyperintense abnormalities on T2-weighted images was 2.0 mL (range, 0.4–4.7 mL) for focal abnormalities, whereas it was 15.5 mL (range, 1.5–39.3 mL) when including diffuse hyperintense abnormalities on T2-weighted images. The average MT ratio of focal lesions was 53.3% (range, 34.1–62.6%). It was 60.5% (range, 51.6–65.0%) when focal and diffuse hyperintense abnormalities were pooled together. Cerebral atrophy was evident at visual inspection in eight patients (mild in five, moderate in two, and severe in one). Cerebellar atrophy was also seen in eight patients (mild in seven and severe in one). An abnormality on MR images was clearly detected in the dentate nuclei and surrounding white matter in seven patients.

Table 1 reports the mean and SD of the whole-brain, NAWM, and NAGM MT ratio histogram–derived metrics for patients with CTX and for control subjects. Average whole-brain, NAWM, and NAGM MT ratio histograms from patients and control subjects are presented in Fig 1. Average MT ratios and peak heights of all three histograms from patients with CTX were significantly lower than the corresponding quantities from the control subjects. Table 2 reports the means and SD of the MT ratio histogram-derived metrics of cerebellar NAGM and NAWM

TABLE 2: Mean MT ratio histogram-derived metrics of cerebellar NAWM and NAGM for the nine patients with CTX and the 10 control subjects

Variable	Control Subjects	Patients with CTX	*P* Value*
NAWM			
MT ratio (%)	61.9 (1.0)	59.1 (2.9)	.01
MT ratio peak height†	170.9 (60.5)	149.2 (82.3)	NS
MT ratio peak position (%)	57.4 (2.0)	57.2 (3.4)	NS
NAGM			
MT ratio (%)	56.3 (0.9)	51.7 (3.8)	.002
MT ratio peak height†	116.9 (20.6)	76.1 (26.6)	.002
MT ratio peak position (%)	52.7 (0.8)	48.4 (1.0)	.01

Note.—Numbers in parentheses are SD.

* NS indicates not significant.

† These data are normalized pixel count.

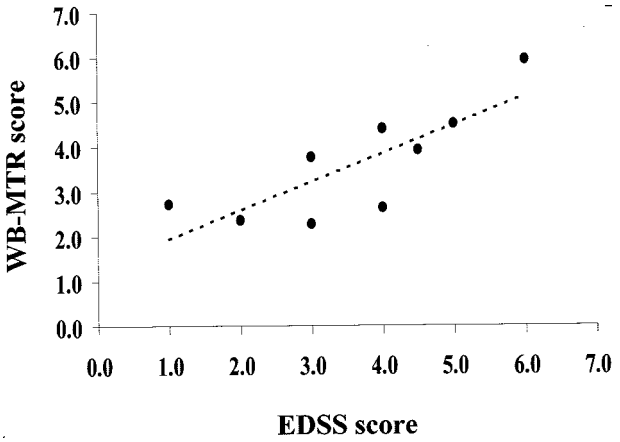

FIG 2. Scatterplot of the correlation between the EDSS score and composite whole-brain (*WB*) MT ratio (*MTR*) histogram score in the nine patients with CTX ($r = 0.77$).

from patients with CTX and from control subjects. NAGM MT ratio histogram–derived metrics from patients with CTX were significantly lower than the corresponding quantities from control subjects. Average MT ratio of the cerebellar NAWM histogram was also significantly different between patients with CTX and control subjects.

Strong correlations were found between the EDSS score and the composite whole-brain MT ratio histogram score ($r = 0.77$, $P < .01$) (Fig 2), and the composite brain white matter MT ratio histogram score ($r = 0.71$, $P < .03$). A moderate correlation was also found between the EDSS score and the composite gray matter MT ratio histogram score ($r = 0.59$, $P < .09$). A strong correlation was found between the cerebellar functional system score and the composite cerebellar NAWM score ($r = 0.72$, $P < .02$). No significant correlations were found between EDSS score and lesion volume or average lesion MT ratio, or between the cerebellar functional system score and composite cerebellar NAGM score.

Discussion

There is an increasing body of evidence that the brain tissue damage in patients with CTX extends well beyond the abnormalities seen on conventional MR images and that the 'occult' component of CTX brain damage contributes to the development of irreversible neurologic disability (8, 9). Nevertheless, the distribution and the nature of this microstructural damage, to our knowledge, have not been investigated yet. In addition, MR imaging markers of disease progression that would enable quantification of overall brain damage in patients with CTX are lacking; such markers might enable accurate monitoring of the evolution of the disease.

Several considerations indicate MT MR imaging as a good candidate to provide new measures of CTX brain damage that will improve our ability to understand and monitor this disease. First, as shown in several neurologic conditions of different origin (15–20, 23), MT MR imaging is sensitive to the most destructive aspects of central nervous system disease (ie, irreversible and severe demyelination and neuronal and axonal loss) that occur both outside and within lesions of the central nervous system that are visible on T2-weighted images. Second, by means of histogram analysis (15–20), MT MR imaging allows the assessment of damage in the whole of the brain tissue, thus avoiding sample biases that are likely to occur when using a region-of-interest–based analysis. Third, extracting information regarding specific tissues (such as NAWM and NAGM) (26) and anatomic regions (such as the cerebellum) from MT MR imaging data is possible (27).

Whole-brain MT ratio histogram analysis from brain tissue provided additional evidence for the presence of diffuse abnormalities in patients with CTX (9). As in other white matter diseases, such as multiple sclerosis (15–17), focal white matter lesions contribute little to whole-brain MT ratio histogram changes. On the contrary, diffusely damaged tissue and normal-appearing tissue represent the largest component of the examined tissue and, as a consequence, are likely to be the major contributors to the observed MT ratio histogram abnormalities. This is of particular importance in patients with CTX, in whom neuronal and mitochondrial dysfunction is known to occur in the normal-appearing tissue (9) and in whom a considerable amount of diffusely hyperintense changes of the white matter exists (5–9), the extension of which is difficult to determine reproducibly on conventional MR images owing to the fuzzy borders of these abnormalities. Consistent with the view that

nonfocal damage of CTX is important in causing neurologic impairment in these patients, we found a strong correlation between the whole-brain MT ratio histogram composite and the EDSS scores. Such a strong correlation between clinical and MT MR histogram findings in CTX indicates that the quantitative assessment of overall brain damage might provide a new powerful approach to monitoring the disease evolution. This is even more important when considering that lesion volume, as also found by others (8), and average lesion MT ratio did not correlate with EDSS score. In addition, the extensive and diffuse involvement of brain tissue fits well with the notion that CTX is a genetic disorder. Similar MT ratio findings were indeed present in patients with other genetic conditions involving the central nervous system, such as Leber hereditary optic neuropathy (28) and nocturnal frontal lobe epilepsy (29).

This study also assessed NAWM and NAGM pathologic changes separately and provided the first, to our knowledge, in vivo evidence that both these tissues are not spared by CTX brain damage. We segmented NAWM from both focal and diffuse hyperintense abnormalities as seen on conventional MR images. As a consequence, the NAWM MT ratio histogram changes are attributable to microstructural damage beyond the resolution of conventional MR imaging, and our results are indicative of a graded but overall white matter structural damage in patients with CTX. The strong correlation found between patients' EDSS scores and brain and cerebellar NAWM changes also suggests that CTX microstructural damage is not negligible in terms of the clinical outcome of the disease. Although this study does not allow for defining the pathologic nature of the microstructural white matter changes of CTX, Wallerian degeneration of fibers passing through the macroscopic lesions of the disease or microscopic damage secondary to local accumulation of cholestanol are two possible but not mutually exclusive factors. We also found that patients with CTX have abnormal NAGM MT ratio histograms. Although we cannot exclude a contribution from CSF partial-volume averaging, particularly in those patients with brain and cerebellar atrophy, this finding fits with the results of previous conventional MR imaging (5–9) and histochemical (30) studies showing that gray matter in patients with CTX is frequently and diffusely involved and with the demonstration of a widespread *N*-acetylaspartate decrease in the brain in patients with CTX (9). Although the relatively small number of patients studied prevented us from finding a significant correlation between the composite NAGM MT ratio histogram and EDSS scores, our findings are consistent with the common and profound cognitive impairment of patients with CTX (2, 4).

Reduced MT ratio histogram–derived metrics indicate a reduction of 'bound' water in the diseased tissue (10). Although we can only speculate on the possible pathologic substrates of these findings, they are likely to reflect two of the major aspects of CTX, that is, nerve cell loss in the gray matter and demyelination and axonal injury in the white matter (31, 32). However, the exact dynamics of the central nervous system damage in CTX remains to be established, since some authors suggest demyelination to be the primary event (33, 34), whereas others propose that the basic enzymatic effect of this disorder may lead to the accumulation of neurotoxic metabolites responsible for a primary neuroaxonal abnormality with secondary myelin loss (31, 32). Given that MT MR imaging is able to depict and to provide separate information about CTX-related changes in white matter and gray matter, the in vivo assessment of tissue damage in early cases of CTX by using serial MT MR imaging might improve our understanding of this important aspect of the disease, which is unlikely to be clarified on the basis of postmortem studies.

Conclusion

MT ratio histogram analysis provided in vivo estimates of CTX brain damage that strongly correlated with the clinical status of the patient. It also provided in vivo evidence that both NAWM and NAGM are not spared by CTX damage. Quantitative assessment of brain damage in patients with CTX by using MT MR imaging has the potential to provide powerful measures of disease outcome and to improve our understanding of CTX pathophysiology.

Acknowledgments

The authors are grateful to Dr M.P. Sormani for her help in conducting statistical analysis.

References

1. Oftebro H, Björkhem I, Stormer FC, Pedersen JI. **Cerebrotendinous xanthomatosis: defective liver mitochondrial hydroxylation of chenodeoxycholic acid precursors.** *J Lipid Res* 1981;22:632–640
2. Verrips A, Hoefsloot LH, Steenbergen CH, et al. **Clinical and molecular genetic characteristics of patients with cerebrotendinous xanthomatosis.** *Brain* 2000;123:908–919
3. Bjorkhem I, Boberg KM. **Inborn errors in bile acid biosynthesis and storage of sterols other than cholesterol.** In: Scriver CR, Beaudet AL, Sly WS, Valle D, eds. *The Metabolic and Molecular Bases of Inherited Disease.* 7th ed. New York: McGraw-Hill, 1995; 2073–2099
4. Federico A, Dotti MT. **Cerebrotendinous xanthomatosis**. In: Vinken PJ, Bruyn GW, Moser HW, eds. *Handbook of Clinical Neurology.* Vol 66. Amsterdam: Elsevier Science, 1996;599–613
5. Berginer VM, Berginer J, Korczyn AD, Tadmor R. **Magnetic resonance imaging in cerebrotendinous xanthomatosis: a prospective clinical and neuroradiological study.** *J Neurol Sci* 1994;122:102–108
6. Dotti MT, Federico A, Signorini E, et al. **Cerebrotendinous xanthomatosis (van Bogaert Scherer Epstein disease): CT and MR findings.** *AJNR Am J Neuroradiol* 1994;15:1721–1726
7. Valk J, van der Knaap MS. **Selective vulnerability in toxic encephalopathies and metabolic disorders.** *Riv Neuroradiol* 1996;9:749–760
8. Barkhof F, Verrips A, Wesseling P, et al. **Cerebrotendinous xanthomatosis: the spectrum of imaging findings and the correlation with neuropathologic findings.** *Radiology* 2000;217:869–876
9. De Stefano N, Dotti MT, Mortilla M, Federico A. **Magnetic resonance imaging and spectroscopic changes in brains of patients with cerebrotendinous xanthomatosis.** *Brain* 2001;124:121–131
10. Filippi M. **In-vivo tissue characterization of multiple sclerosis and other white matter diseases using magnetic resonance-based techniques.** *J Neurol* 2001;248:1019–1029
11. Berginer VM, Salen G, Shefer S. **Long-term treatment of cerebrotendinous xanthomatosis with chenodeoxycholic acid.** *N Engl J Med* 1984;311:1649–1652

12. Pedley TA, Emerson RG, Warner CL, Rowland LP, Salen G. **Treatment of cerebrotendinous xanthomatosis with chenodeoxycholic acid.** *Ann Neurol* 1985;18:517–518
13. Verrips A, Wevers RA, van Engelen BG, et al. **Effect of simvastatin in addition to chenodeoxycholic acid in patients with cerebrotendinous xanthomatosis.** *Metabolism* 1999;48:233–238
14. van Waesberghe JHT, Kamphorst W, De Groot CJA, et al. **Axonal loss in multiple sclerosis lesions: magnetic resonance imaging insights into substrates of disability.** *Ann Neurol* 1999;46:747–754
15. van Buchem MA, McGowan JC, Kolson DL, Polansky M, Grossman RI. **Quantitative volumetric magnetization transfer analysis in multiple sclerosis: estimation of macroscopic and microscopic disease burden.** *Magn Reson Med* 1996;36:632–636
16. Filippi M, Iannucci G, Tortorella C, et al. **Comparison of MS clinical phenotypes using conventional and magnetization transfer MRI.** *Neurology* 1999;52:588–594
17. Filippi M, Inglese M, Rovaris M, et al. **Magnetization transfer imaging to monitor the evolution of MS: a 1-year follow-up study.** *Neurology* 2000;55:940–946
18. Iannucci G, Dichgans M, Rovaris M, et al. **Correlations between clinical findings and magnetization transfer imaging metrics of tissue damage in individuals with cerebral autosomal dominant arteriopathy with subcortical infarcts and leucoencephalopathy.** *Stroke* 2001;32:643–648
19. Rovaris M, Viti B, Ciboddo G, et al. **Brain involvement in systemic immune-mediated diseases: a magnetic resonance and magnetization transfer imaging study.** *J Neurol Neurosurg Psychiatry* 1999;68:170–177
20. Bozzali M, Franceschi M, Falini A, et al. **Quantification of tissue damage in AD using diffusion tensor and magnetization transfer MRI.** *Neurology* 2001;57:1135–1137
21. Kurtzke JF. **Rating neurological impairment in multiple sclerosis: an Expanded Disability Status Scale (EDSS).** *Neurology* 1983;33:1444–1452
22. Studholme C, Hill DLG, Hawkes DJ. **Automated 3D registration of MR and PET brain images by multi-resolution optimisation of voxel similarity measures.** *Med Physics* 1997;24:25–35
23. Tortorella C, Viti B, Bozzali M, et al. **A magnetization transfer histogram study of normal-appearing brain tissue in MS.** *Neurology* 2000;54:186–193
24. Rovaris M, Filippi M, Calori G, et al. **Intra-observer reproducibility in measuring new MR putative markers of demyelination and axonal loss in multiple sclerosis: a comparison with conventional T2-weighted images.** *J Neurol* 1997;244:266–270
25. Ashburner J, Friston KJ. **Multimodal image coregistration and partitioning: a unified framework.** *Neuroimage* 1997;6:209–217
26. Cercignani M, Bozzali M, Iannucci G, Comi G, Filippi M. **Magnetisation transfer ratio and mean diffusivity of normal appearing white and grey matter from patients with multiple sclerosis.** *J Neurol Neurosurg Psychiatry* 2001;70:311–317
27. Iannucci G, Minicucci L, Rodegher M, Sormani MP, Comi G, Filippi M. **Correlations between clinical and MRI involvement in multiple sclerosis: assessment using T1, T2 and MT histograms**. *J Neurol Sci* 1999;171:121–129
28. Inglese M, Rovaris M, Bianchi S, et al. **Magnetic resonance imaging, magnetisation transfer imaging, and diffusion weighted imaging correlates of optic nerve, brain, and cervical cord damage in Leber's hereditary optic neuropathy.** *J Neurol Neurosurg Psychiatry* 2001;70:444–449
29. Ferini-Strambi L, Bozzali M, Cercignani M, Oldani A, Zucconi M, Filippi M. **Magnetization transfer and diffusion-weighted imaging in nocturnal frontal lobe epilepsy.** *Neurology* 2000;54:2331–2333
30. Stahl WL, Sumi SM, Swanson PD. **Subcellular distribution of cerebral cholestanol in cerebrotendinous xanthomatosis.** *J Neurochem* 1971;18:403–413
31. Pop PH, Joosten E, van Spreeken A, et al. **Neuroaxonal pathology of central and peripheral nervous system in cerebrotendinous xanthomatosis (CTX).** *Acta Neuropathol (Berl)* 1984;64:259–264
32. Soffer D, Benharroch D, Berginer V. **The neuropathology of cerebrotendinous xanthomatosis revisited: a case report and review of the literature.** *Acta Neuropathol (Berl)* 1995;90:213–220
33. Philippart M, van Bogaert L. **Cerebrotendinous xanthomatosis: a generalized disorder of cholestanol metabolism.** *Trans Am Neurol Assoc* 1969;94:322–324
34. Elleder M, Michalec C, Jirasek A, Khun K, Havlova M, Ranny M. **Membranocystic lesion in the brain in cerebrotendinous xanthomatosis: Histochemical and ultrastructural study with evidence of its ceroid nature.** *Virchows Arch B Cell Pathol Incl Mol Pathol* 1989;57:367–374